Proc. Estonian Acad. Sci. Phys. Math., 2007, **56**, 2, 177–196
https://doi.org/10.3176/phys.math.2007.2.14

Phase metastability in shape memory alloys. Dampers in engineering via SMAs

Vicenç Torra[a], Antonio Isalgué[a], Francisco C. Lovey[b], and Ferran Martorell[a]

[a] CIRG-DFA-ETSECCPB, Polytechnical University of Catalonia, Campus Nord B4-B5, E-08034 Barcelona, Catalonia, Spain; vtorra@fa.upc.edu
[b] Centro Atómico de Bariloche and Instituto Balseiro, 8400 S.C. de Bariloche, Argentina

Received 15 January 2007

Abstract. The particular properties of shape memory alloys (SMAs) are related to a martensitic transformation between metastable phases. Their applicability to dampers in civil engineering requires a fully guaranteed behaviour of the SMAs both on mesoscopic and atomic levels. The first one relates the thermomechanical properties (fracture, number of working cycles, summer–winter temperature effects and, for instance, self-heating associated with latent heat and the frictional work converted on heat) and the second one, the actions on the phase transition of the thermodynamic forces (temperature and stress). The properties of the CuAlBe alloy are explained and the characteristics of the NiTi alloy are outlined. By establishing an appropriate model the SMA dampers are introduced inside a structure and, via the ANSYS software, the dynamic response of the free and of the damped structure are obtained by simulation under the action of acceleration from the earthquakes available in the literature. As a conclusion, the conditions for the appropriateness of the dampers are given.

Key words: dampers, shape memory alloy, thermomechanical treatments, diffusion, phase transition, martensitic transformation, metastable phases.

1. INTRODUCTION

The particular properties of shape memory alloys (SMAs) are related to a martensitic transformation between metastable phases (see [1] and references therein). The use of SMAs for damping scarce oscillations during 1–2 min (e.g., as in earthquakes) after several years (or decades) of complete inactivity differs from damping vibrations in satellite launching with two to five acceleration steps in two weeks (normally fresh material is used), or in stayed cables for bridges under wind and rain interactions with several thousands of oscillations each day

in, for instance, wet ambient. Classical analysis of SMAs requires determination of the working life of the alloy: amplitude and cycle number to fracture, changes in the hysteretic behaviour in internal or partial loops, temperature effects induced by self-heating or external summer–winter temperatures under the action of the Clausius–Clapeyron equation and, also, creep effects changing the length of the damper. The particular effects of metastability (or nonclassical effects) require deep analysis in the needed timescale of the application and, also, according to the thermomechanical requirements.

In damping, the mechanical formalism suggests that the efficiency increases when the material always works inside the hysteresis cycle, making internal loops. Working in the phase coexistence zone requires that the metastability should not induce particular changes in the material behaviour, i.e., those related to atomic diffusion in parent, martensite or in the phase coexistence. In other words, the thermodynamic force (stress and temperature) needs to be considered. In fact, the mechanical analysis suggests the use of "pre-stressed" dampers. Certainly, the mechanical efficiency is enhanced, but when the SMA is held in the coexistence zone for several decades, the atomic diffusion can modify the material state. In Cu-based alloys the classical martensite stabilization appears, modifying the hysteretic behaviour. Also, preliminary studies of the NiTi alloy under the stress and temperature effects show changes in the level of the transformation and retransformation stresses.

The use of SMAs in earthquake dampers, situated in the diagonals of the porticos [2–4] during scarce but, eventually, intense events after several decades without any action, requires also the knowledge of the life to fracture. As the quake action is time-limited (1–2 min), the number of oscillations required for one structure with frequencies close to 1 Hz is between 100 and 200. This amount of cycles is easily attained for polycrystalline NiTi or Cu-based alloys. Thus the main challenge is obtaining a material where the relevant properties are stable with time without SMA creep accumulation.

The transformation process itself in Cu-based and in NiTi alloys uses different mesoscopic mechanisms. In the CuAlBe alloy the transformation (usually distributed) takes place progressively in the sample mass. In NiTi polycrystalline wires, the process is frequently related to "band zones" similar to that observed in the CuZnAl single crystal [1]. The macroscopic effect is a different local self-heating mechanism. In CuAlBe the transformed zones include part of the material in the parent phase, in NiTi the transformation is mainly induced by a transformation front (similar to Ludders bands) associated with local transformation.

The development of an application as dampers for quakes requires three levels of description [1–4], two of which are associated with SMA material particularities and the last one is related to simulation of the damper situated inside the structure under the action of quake accelerations. **The first level** relates the mesoscopic properties of SMAs (Cu-based and NiTi alloys) oriented to dampers. In dampers, situated in the diagonals of the porticos, the accumulative and progressive

permanent deformation in cycling (SMA creep) needs to be avoided: an appropriate experimental approach to thermomechanical treatment is required. **The second level** is associated with microscopic effects (atomic diffusion induced by temperature or stress) and the estimated timescales. The observations for the NiTi alloy suggest that the use of phase coexistence and/or temperature actions associated with direct sunny influence on the alloy seems inappropriate. **The third level**, via the experimental analysis and under the constraints induced by the ANSYS software, is centred on building an appropriate model in ANSYS via a proprietary subprogram (an ANSYS routine USERMAT). From the outline of the family house structure with some SMA dampers, the effects of the accelerations for several quakes show that the SMA damper is able to reduce the oscillation amplitude to the half.

In this work a complete solution for dampers of family houses via SMAs is outlined. The appropriate heat treatment for CuAlBe polycrystalline alloys is summarized. The material avoids permanent deformation for strains near 4%. The self-heating effects are also qualitatively evaluated. Some microscopic evolution in lengthy timescales is outlined for CuAlBe and, furthermore, for the NiTi alloy. The experimental hysteresis cycle is modelled in terms of a set of parallel bilinear elements with satisfactory agreement with the experimental internal loops. The model, via a proprietary USERMAT routine, is inserted inside ANSYS. Using the structure of a family house, the behaviour of a free (elastic) and damped structure is simulated on the basis of quakes extracted from the literature. For quakes, such as “El Centro” close to 7 in the Richter scale, the main goal of the dampers introduced in the structure is to keep the oscillation amplitude always under half of the behaviour without dampers and/or under the plastic limit of the structure.

2. SMA PROPERTIES FOR DAMPERS IN FAMILY HOUSES

Figure 1 shows a family house with a surface close 200 m^2, with loads near (or under) 100 kN. In Fig. 1b, the structure is outlined, with the dampers situated in the portico diagonals. The structure can be treated, eventually, by two semi-independent volumes: one floor part plus two floor parts with or without connection. Preliminary analysis requires, also, the study of the “independent” portico situated in the structure (see section 4).

The requirements, 10 to 20 years without any relevant changes of the main properties, suggest the passive state of the SMA to be in the parent (beta) phase. Ensuring reproducible behaviour of the SMA requires that the work be performed inside the pseudo-elastic window (PEW; see Fig. 2) without overcoming the limits associated with plastic deformation. The available stress is between $\sigma = 0$ and $\sigma = \sigma_{pd}$, the deformation between $\varepsilon = 0$ and $\varepsilon = \varepsilon_{max}$, and the temperature between slightly above T_1 and T_2. At zero stress the transformation temperature is Ms (or martensite start temperature), and $\Delta\sigma_h$ is hysteresis width.

(a) (b)

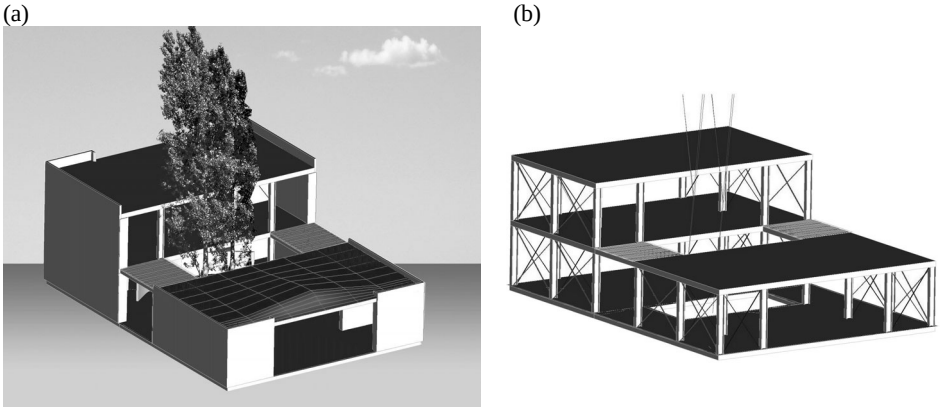

Fig. 1. (a) External view of the sample family house with an internal garden in the ground and, also, in the roof of the first floor. (b) Structural sketch of the house.

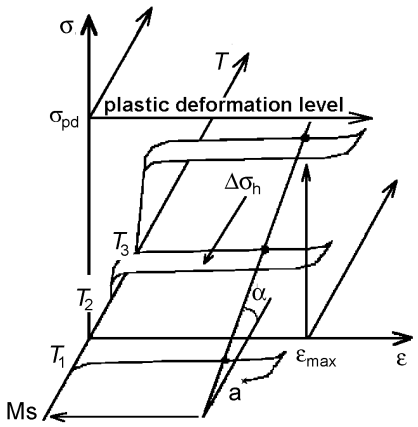

Fig. 2. SMA behaviour in stress (σ), strain (ε), and temperature (T) representation. The pseudoelastic window is comprised inside the temperature interval corresponding to the plastic deformation level in transforming, the temperature at which complete reversion of strain is achieved on unloading (if the sample is deformed at a lower temperature than T_1, the unloading path may cross the 0 strain plane, as indicated by point **a**, avoiding the return to the parent phase and losing the self-centring capabilities), and strains lower than ε_{max}.

The level of fracture in the CuAlBe alloy “as furnished” is close to 300–350 MPa. After heat treatment at 1123 K the grain diameter is greatly increased (Fig. 3), material in the parent phase is obtained, and the alloy strength is reduced to 250–300 MPa.

The behaviour, after a classical heat treatment for 2 min at 1123 K and 1 h of ageing at 373 K (see Fig. 4), shows a relevant and progressive SMA creep. In fact, the experimental SMA creep indicates that the alloy, in this condition, is inappropriate for use in dampers. The macroscopic working behaviour is changed after the ageing and an efficient thermomechanical treatment at 373 K and 323 K (see Fig. 5).

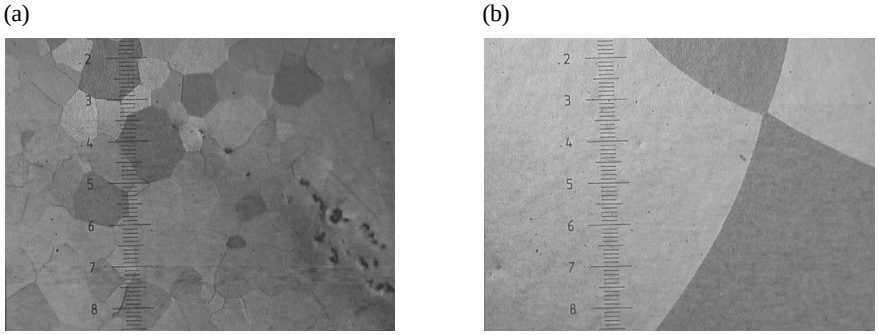

Fig. 3. Increase in the grain diameter after heating for 40 min at 1123 K (vertical scale of micrographs near 0.7 mm): (a) material as furnished; (b) material after the heat treatment.

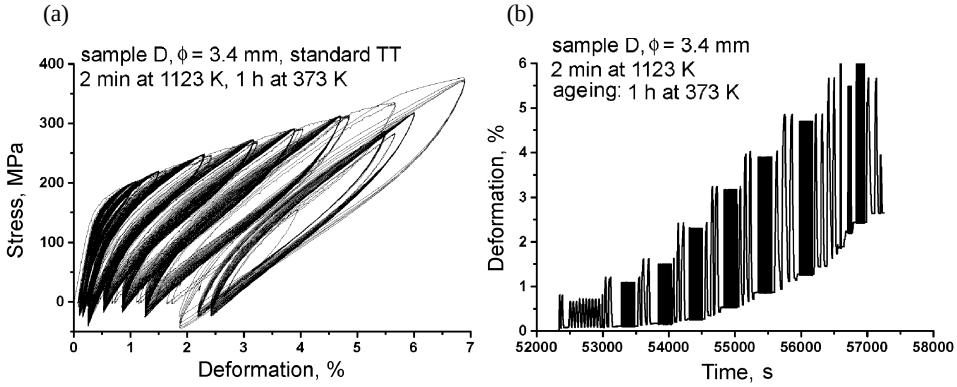

Fig. 4. Stress–strain (a) and strain–time (b) relationship of cycling showing a progressive SMA creep associated with a series of cycles of progressive amplitude.

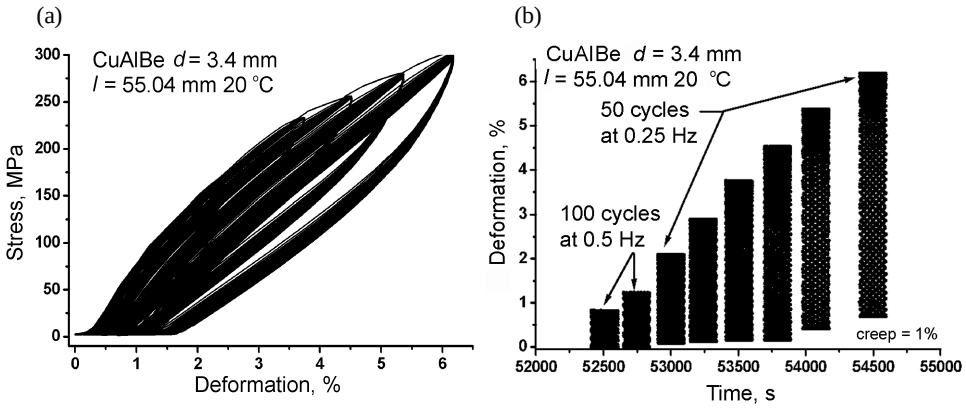

Fig. 5. Stress–strain (a) and strain–time (b) relationship of progressive cycling after an appropriate homogenization at 1123 K, quenching, ageing, and thermomechanical treatment.

The homogenization time, the appropriate ageing, and the efficient thermomechanical treatment show that the alloy permits series of cycles without SMA creep for deformations up to 4.5% (Fig. 5). The thermomechanical heat treatment is adapted to the CuAlBe alloy: the main effect of the thermomechanical treatment is that the stabilized stress-induced martensite is suppressed. In fact, the parasitic effects of the treatment disappear for deformations under 4.5%. The CuAlBe alloy, starting in the parent phase, is appropriate for work in dampers ensuring the 100–200 necessary cycles.

On cycling, the transformation–retransformation process induces a self-heating by the latent heat and a progressive increase in temperature related to the work (the hysteresis cycle), converted into heat. The effects are particular for each alloy. The self-heating is more important in NiTi than in CuAlBe. Figure 6a shows the temperature effects in a CuAlBe wire (diameter 3.4 mm) for several amplitudes and frequencies. A similar measurement was performed with a wire of NiTi (diameter 2.46 mm). The comparison indicates that the temperature oscillation is close to 15 K in NiTi but close to 4 K in CuAlBe. The difference is due to several effects, particularly the latent heat and the transformation mechanisms: usually NiTi transforms "completely" by bands or zones, and CuAlBe progressively (distributed transformation). In the latter, the heat is distributed in the complete mass of the available material. The difference in nucleation and growth produces great difference in the temperature oscillations.

An appropriate behaviour simulation requires the consideration of the self-heating and, also, the effect of external temperature as, for instance, the temperature changes associated with night and day, and summer and winter. As Fig. 2 qualitatively shows, an increase in temperature implies that the transformation stress becomes more intense according to the Clausius–Clapeyron coefficient (CCC) associated with any phase transformation. The thermodynamic analysis to evaluate the CCC requires experimental conditions where the state of the material

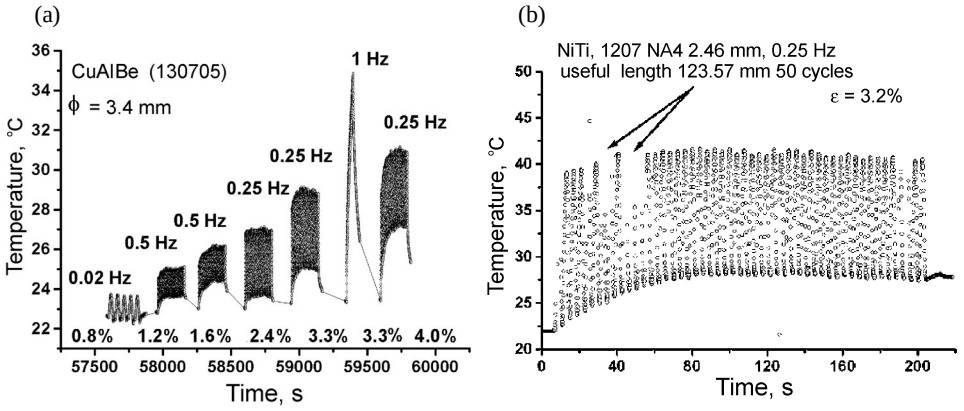

Fig. 6. Temperature effects in SMAs. (a) Cycling for series of cycles of progressive amplitude in CuAlBe. (b) An example for a NiTi wire; the arrows indicate that some experimental readings are incorrect due to movement of thermocouple.

remains unchanged, when transformation cycles at different temperatures are performed. In the CuAlBe polycrystalline material, the condition is fully satisfied when the hysteretic cycles, obtained at different temperatures, are carried out with deformations under 3–4%, where the SMA creep is not relevant (experimental value 2.2 MPa/K). In NiTi the situation is somewhat different: parasitic effects of the R-phase cannot be avoided at low stresses. At high stresses, there is creep. It is recommended to "train" the specimen with several cycles at a "higher temperature" and, later, perform a set of measurements at a progressive lower temperature with the same deformation amplitude. The stress value is measured at the inflexion point $(\partial^2\sigma/\partial\varepsilon^2 = 0)$ on loading (experimental value: 6.3 MPa/K).

3. DIFFUSION EFFECTS

Resistance measurements against time and temperature permit analysis of the CuAlBe behaviour after quenching and ageing. Figure 7 shows the evolution of the transformation temperature (Ms) on ageing obtained from resistance measurements against time. The curve presents, after the initial quenching procedure, the ageing evolution of Ms at 373 K for 110 days and at 353 K until 250 days. After 250 days of this "initial ageing" we observe that the Ms tracks the external temperature (a: 373 K, b: 353 K, and c: 363 K) in a reproducible manner (from day 250 to day 400) [2–4]. This behaviour can be described by an exponential relationship with a time constant related to the activation energy. Figure 7 shows that around 353 K any temperature step requires about six months to reach the steady state. At room temperature the evolution practically remains under the available resolution of resistance measurements (usually four or five significant figures in long-time resistance measurements). In the initial part of the ageing (at 373 K) the Ms evolution is also related to after quench phenomena.

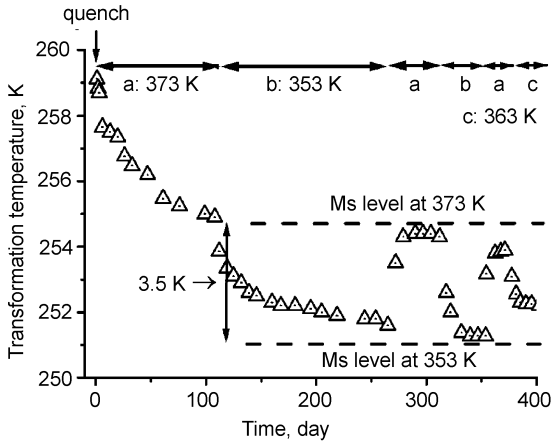

Fig. 7. The evolution of the transformation temperature (Ms) in ageing after a quench in water (from 1123 K to 293 K) for the CuAlBe alloy.

Table 1. Mesoscopic and microscopic (diffusion) effects on a CuAlBe alloy

Material properties (CuAlBe alloy)	Temperature variation
Hysteresis width	30–50 K
Summer–winter temperature change (CCC)	20 K
Self-heating	10 K
After quench Ms change	5 K
Phase coexistence	−10 K
Summer–winter tracking (atomic order)	3 K
Security domain	20 K
Global effect	100 K (or 220 MPa)

The material is influenced by a set of mesoscopic (i.e., room temperature changes or self-heating under the action of the CCC) and microscopic phenomena as the Ms tracking with ageing temperature and time. Some of them induce opposite actions. For instance, at low cycling frequency (e.g., in wires with the diameter under 1 mm and frequencies lower than 0.1 Hz) the maximum stress decreases with cycling (effect due to the phase coexistence effect) but, with increase in the frequency the dissipated heat compensates and even overcomes the previous effects increasing progressively the maximum stress. Table 1 shows the direct estimated temperature changes for each action, or case, or the equivalent effects for the stress increase via the CCC. It is assumed that the temperature of the damper surroundings would be that of the house inside, i.e., without direct contact with external ambient or sunlight. Changes from summer to winter in a range of about 20 K are considered as a typical case.

The experimental analysis indicates that the CuAlBe alloy suits for dampers in family houses. The life to fracture is longer than the 100–200 necessary cycles. The suppression of the parasitic effects, associated with martensite stabilization, requires the damper to remain in the parent phase during the eventually long passive period.

3.1. Some remarks on the NiTi alloy

The self-heating in NiTi was evaluated for some particular cases, as shown in Fig. 8 for a wire with 2.46 mm diameter. It can be seen that deformations near 5% induce heating close to 35 K. As the CCC in the alloy is close to 6.5 MPa/K, the supplementary stress increase overcomes 200 MPa and the material can fall in the plastic deformation domain, producing a relevant SMA creep on cycling.

The NiTi alloy is highly sensitive to temperature. Figure 9 shows the SMA creep at relatively higher stresses (temperature 325 K) for a wire of 2.46 mm diameter. On cycling the SMA creep and the evolution of the cycle shape are highly relevant. In fact, the initial shape, close to rectangular (or appropriate for bilinear models) evolves to a hysteresis cycle similar to the CuAlBe alloy (see the end of section 4).

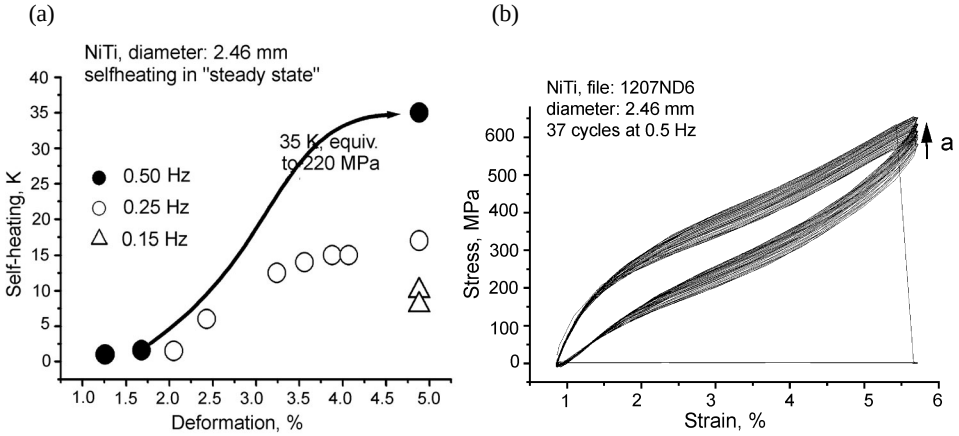

Fig. 8. Self-heating effects in the NiTi alloy. (a) Associated temperature effects related to cycling frequency and deformation. (b) Self-heating associated to stress–strain cycles. The arrow (**a**) shows the progressive increase in the maximal loading by a series of "fast cycles" with deformation close to 5%.

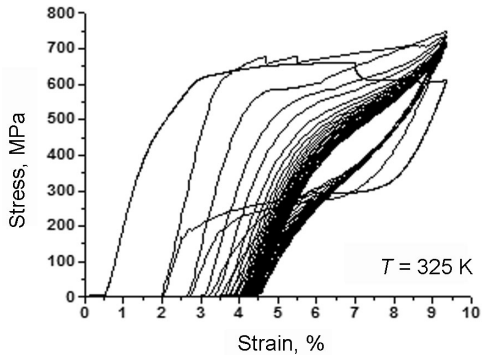

Fig. 9. Series of cycles in NiTi at 325 K. When the stress overcomes 600 MPa, the progressive permanent deformation modifies the hysteresis cycle and increases the SMA creep.

NiTi alloys are relatively stable at room temperature. However, their properties evolve noticeably by ageing at a little higher temperature. Figure 10 shows the effects of ageing at 373 K on the calorimetric response, basically in the R-phase domain.

Time effects are also observed in the martensite phase (stabilization), and also minor effects in the parent phase and in the phase coexistence (parent and martensite). The effects at extremely long time suggest that the use of NiTi under direct sun influence cannot be avoided after 10–20 years, as suggested by Fig. 10. The effects for other applications need to be studied according to their particular needs. For instance, in damping of stayed cables the main requirement is the number of working cycles: several tens of thousands or more per day. Direct measurements using wires with 2.46 mm diameter and deformation around 3–4% suggest that the fracture on cycling might take place under 10 000 cycles.

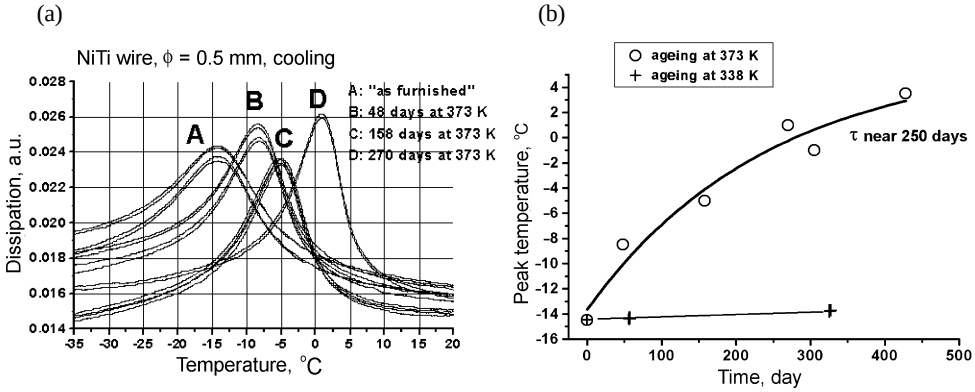

Fig. 10. Ageing effects on the NiTi alloy. (a) Effects on the calorimetric curves of 0, 48, 158, and 270 days at 373 K. (b) Peak temperature against time for 373 K and 338 K.

4. SMA MODEL FOR STRUCTURAL SIMULATIONS

Modelling the SMA behaviour is a complex topic of permanent interest (see [1] and related references and [4–11], for several recent approaches). The inherent complexity of the martensitic transformation of the SMA requires a formulation at various depth levels (stiffness, phase transformation, thermal effects, diffusion). The importance of each level depends on the requirements which are to be satisfied by the material in the working situations. Each material presents several different timescales. There are fast effects related to thermo-mechanical oscillations governing the damping actions under earthquake effects, and slow effects governed by atomic diffusion that determine the material lifetime and usefulness. All these effects must be considered when designing damping applications for civil engineering. We have developed one-dimensional (1D) models, especially considering traction, temperature, and diffusion effects, which are the most relevant effects for our application [1]. The first 1D model that considers the most relevant physical effects was developed for a CuAlZn single crystal [4]. The model is built from observations on SMA single crystals, which transform from the beta to martensite phase with small distributed transformation domains along the sample. The model mimics the physical transformation structure of a single crystal (and roughly of polycrystalline material). For this reason, it is built by a large number (500–1000 elements) of similar elements or domains.

The mechanical representation of phase transition describes the martensitic transformation from the phenomenological data in the intrinsic parameters. The classical nucleation and growth of the phase transformation (Fig. 11) for each element of the wire (or bar) under the action of the external thermodynamic forces (stress and temperature) are considered. The plot illustrates the different paths described when cycling under the effect of an external force. For example, the path (1-2-3-4-5-6-7-8-9-1) corresponds to a complete cycle with nucleation

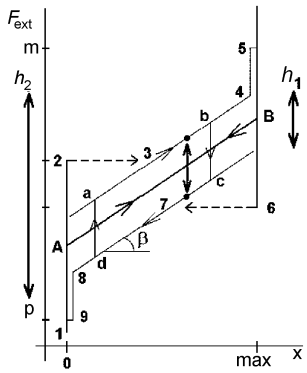

Fig. 11. The mechanical hysteresis cycle defines a single transformation domain. Starting in P (parent phase) at low stress and increasing stress, the transformation to martensite (m) produces a transformation strain. Total (1-2-3-4-5-6-7-8-9-1), partial (1-2-3-b-c-8-9-1), and internal (a-b-c-d-a) cycles are depicted. The CSRT position (A) depends on thermal and atomic diffusion phenomena.

(2-3) and growth (3-4) on transforming, and also nucleation (6-7) and growth (7-8) on retransforming. This path has a maximum hysteresis width h_2. The trajectory a-b-c-d-a represents an internal loop with a minimum hysteresis width h_1. The critical stress of reversible transformation (CSRT) – point A in the plot –, which places the whole cycle in the force axis, characterizes the hysteresis cycle. The CSRT is affected by the temperature and atomic state of the material, thus linking the mechanical actions with the thermal and diffusive phenomena.

This model is a 1D distributed model. The global hysteresis cycle of the sample is the result of the behaviour of the set of elementary transformation domains; one for each martensite plate [1,12], with a statistical scatter in its defining parameters. Using this approach, the calculation of the model is relatively simple. It only involves the addition of simple element responses instead of a complex global function.

4.1. Model implementation for dynamic structural simulations

A detailed model built from an array of transformation domains is able to predict accurately the long-time evolution, including the dynamic effects of SMAs [1,12]. However, the computational load is too high for complex structural simulations (movements of the structure) which include several dampers. We use the predictions of this model to calculate the initial state of the sample for a given simulation. In fact, three initial states are calculated: at standard, low, and high temperatures. Using this information, the material response in all working conditions can be modelled by a simplified model, specially developed for structural simulations. This model is developed for polycrystalline CuAlBe and NiTi alloys. It is composed of a set of parallel transformation domains. The parallel configuration is appropriate for simulation environments, like in ANSYS,

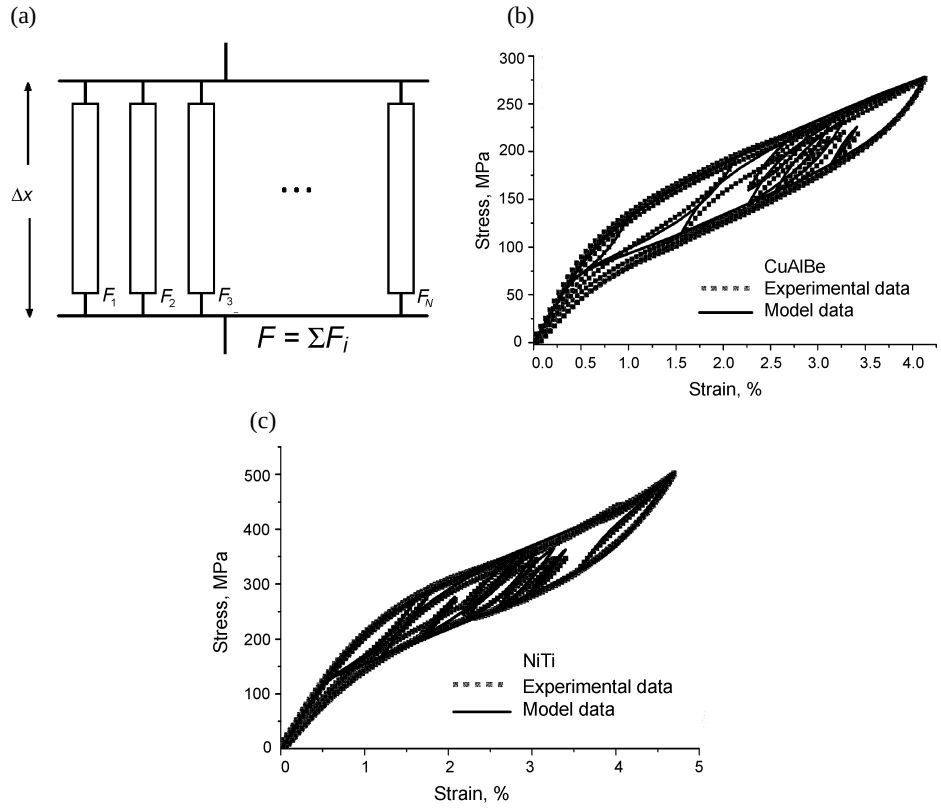

Fig. 12. Model with 9 parallel elements. (a) Sketch of the model construction. (b) Experimental and simulated behaviour of a CuAlBe sample. (c) Experimental and simulated behaviour of a NiTi sample.

where elongation is the element input parameter. Besides, this structure is particularly valid for polycrystalline alloys, as has been reported for similar materials [13]. In the present examples, the model is composed of only 9 parallel elements, which give appropriate results as compared to mechanical test (Fig. 12a). Figure 12 shows the model predictions and the experimental data for CuAlBe (b) and NiTi (c). Temperature changes are calculated using the CCC. The model accuracy for global, partial, and internal cycles is very good and has a reduced computation time. Also, a simpler model for NiTi slow cycling has been developed, based on the bilinear theory (which is widely used for NiTi [7]). However, the error is important, especially when internal loops are present. Furthermore, the computational time for the proposed parallel model is similar to the bilinear model.

5. SIMULATIONS OF EARTHQUAKE ACTIONS

A SMA damper may be simply a wire or rod of material that, due to its hysteresis cycle, is able to convert mechanical energy into heat. In principle, we may use a single SMA rod with an appropriate thickness to endure the stress in the structure. However, there are several reasons that suggest the use of a set of thinner SMA wires instead. First, to be able to use the material, it is necessary to prepare the sample with an appropriate thermomechanical treatment (section 3). This sample preparation loses its efficiency when the thickness of the sample increases (the sample thickness imposes a temperature gradient in the betatization process that prevents Ms homogenization). Second, the grain structure complexity grows with the sample thickness. This increases the undesired material behaviour, for instance, in quenching, which modifies the hysteresis shape (see Fig. 4). For these reasons, we propose a damper structure with N thin wires with a diameter less than 5 mm (Fig. 13). Obviously, this configuration only allows the dampers to work in traction. No compression work is achievable. To overcome this limitation, the dampers always work in pairs on a counteracted geometry.

The design and optimization of the dampers consist of determining the best length and number of wires that compose the damper in a given structure. We are using CuAlBe wires with a diameter of 3.4 mm, able to undergo a stress of 2.5 kN with an ultimate strain above 6% (4.5% without SMA creep), and NiTi wires with a diameter of 2.46 mm with similar stress and strain maximum levels. To ensure an appropriate response of the dampers, we consider only strains up to 3.5–4%. This limitation has two aims: to reduce the accumulated creep and to provide a safety margin. The calculation of the maximum strain and stress for each damper requires the analysis of the structure under the simulated effects of an earthquake. By studying the free oscillation of the building we obtain the free oscillation amplitude, the stresses induced in the structure, and from the steel properties the maximum deformation the structure can undergo without plastic deformation. From the free oscillation amplitude we determine the length of the SMA wires in order to not overcome the maximum expected strain in the SMA with stresses under plastic deformation. We calculate the number of wires required to produce a total stress around 10–30% of the stresses induced in the

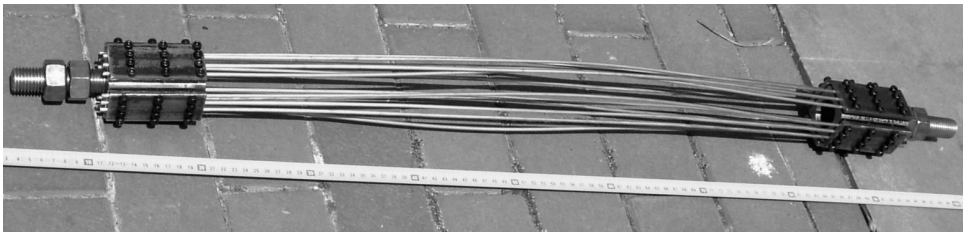

Fig. 13. A SMA damper built from 12 CuAlBe wires with a diameter of 3.4 mm.

structure by the event, expecting a significant action of the dampers with this choice. Usually, starting from these data, a trial and error iterative process is required to fully optimize the dampers.

5.1. Application of SMA dampers in light civil structures

Due to characteristics of SMA dampers (forces below 100 kN and displacements of few centimetres to have a reasonable damping size), light structures are good candidates to use these damping devices. A family house design according to construction standards in Barcelona has been used to study the performance of the designed SMA dampers. The house is composed of two attached sections. The main living area has two storeys of 75 m^2 (11.5 m $\times$ 6.6 m) each. The height of each floor is 3 m. The front section is a single floor structure with a garden on its roof. Its dimensions are 11.5 m $\times$ 6.6 m. The middle section joins both structures with the ground level garden, so the structural coupling between both main sections is small. The structure of the house is made using high-quality steel (A570 grade 50 steel with Young modulus 206 GPa, density 7850 kg/m^3, yield stress of 344 MPa and damping coefficients $\alpha = 0.01$ and $\beta = 0.001$) to improve its response to earthquakes. The house and its beam structure are depicted in Fig. 11.

Several sections of this house have been studied for application of the SMA dampers. Table 2 shows the characteristics of the designed dampers (the number of dampers $\times$ numbers of wires per damper $\times$ wire length), its performance (maximum displacement under free oscillation vs. damped oscillation when the house is excited by the NS component of the "El Centro" earthquake), the quantity of the SMA required to build the dampers and its cost (only raw SMA cost). The table covers three different parts of the house: the triple portico with the highest load in the front section (elevated garden), the entire frontal section, and the entire living area (two-storey section). Figure 14 shows these structures and the position of the dampers in the structure. The results indicate that the dampers are able to reduce the maximum displacements in the structures to half of the free oscillation situation (without dampers) at a competitive cost.

Table 2. Description of the damping system designed for each studied structure. Detail of dampers, cost, and performance

Structure	Damping set	Maximum oscillation, cm	Material mass, kg	Material cost, €
Triple portico	$4 \times 25 \times (0.6 + 0.1)$	7.3/3.1	4.8	480
Garden (single floor)	$12 \times 22 \times (0.38 + 0.1)$	4.3/2.4	8.6	860
Two-storey section	$12 \times 20 \times (0.45 + 0.1)$	6.8/3.0	18.2	1820
	$12 \times 15 \times (0.65 + 0.1)$	15.7/7.1		

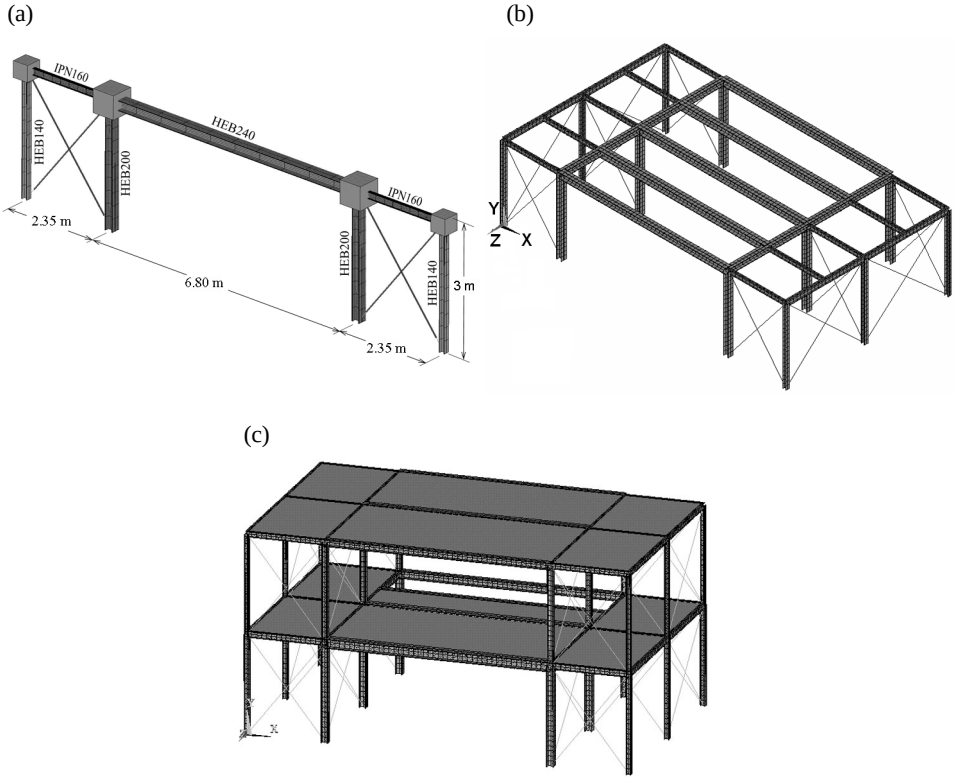

Fig. 14. (a) Beam structure for the garden section with the placement of SMA dampers. (b) Schematic description of the garden central triple portico with "H" cross section pillars (vertical) and "I" cross section beams (horizontal) steel elements, the distributed loads and the SMA damper situation. (c) Double floor beam model used in simulations.

5.2. Detailed application example: two-storey building

To illustrate further the response of the dampers, we include a detailed explanation of the response of the damping system designed for the living area of the house. We use the ANSYS program to perform the structural simulations with the model specially created for simulating the dampers response. For this analysis we use the first 15 s of the "El Centro" north–south component as depicted in Fig. 15a [[14]]. The structure response is shown in Fig. 15b. The maximum displacements induced in the structure are 6.8 cm (1st floor, ceiling) and 15.7 cm (2nd floor or roof), which overcome the plastic deformation limits of the steel beams (5 cm and 6 cm relative displacements for the 1st and the 2nd floor, respectively), and so the building would be damaged by this earthquake (Fig. 16).

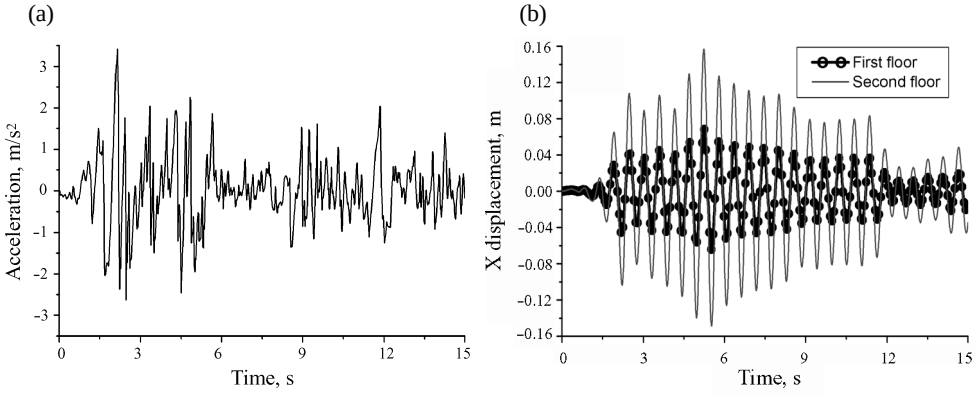

Fig. 15. (a) "El Centro" accelerogram. (b) Free oscillation response for the first and the second floor.

5.2.1. Damping system design

The dampers are placed in the diagonals of the minor arches of the triple porticos as depicted in Fig. 14. We evaluate the response only in the X-axis (longest dimension). Using the described procedure for optimizing the dampers, we calculate 12 dampers of 20×0.45 m (number of wires $\times$ length) for the first floor and 12 dampers of 15×0.65 m. The total amount of CuAlBe is 18.2 kg with an approximated cost of €1820 for extruded wires. Figure 16a shows the oscillations induced in the structure with dampers installed. The maximum peaks are reduced to 3.0 cm and 7.1 cm (1st and 2nd floor, respectively) and the large oscillations are quickly reduced. Figure 16b outlines the dampers response under the earthquake. The dampers do not overcome the strain limit of 4% at 373 K, keeping a security margin. Finally, Fig. 16c shows the energies involved in this event. Initially the energy absorbed by the structure grows quickly. When the oscillations are big enough to induce the martensitic transformation, the dampers start to dissipate energy and the kinetic energy is reduced.

These results indicate the nominal performance of SMA dampers. However, it is necessary to ensure a correct behaviour in the worst conditions. The worst conditions include high external temperatures, self-heating, and atomic evolutions, which are evaluated in the previous sections of this paper. Detailed modelling of these factors requires a complex model outlined in section 4. However, we easily evaluate the system robustness by taking into account the maximum possible value for these variables and considering the worst case constant effect (i.e., the self-heating associated with continuous cycling at 0.25 Hz induces a maximum increase in temperature of 10 K, and then we consider the sample constantly heated up to this temperature). We evaluate all the phenomena to increase the nominal working temperature by 40 K which is a realistic value (see Table 1). Figure 17a,b compare the damped oscillations at nominal temperature (T_{nom}) and at $T_{\text{nom}} + 40$ K. The maximum peaks in these worst conditions are 3.6 and 8.2 cm (1st and 2nd floor, respectively), which still approaches a 50% reduction and keep the steel below its plastic deformation limit showing the robustness of the dampers.

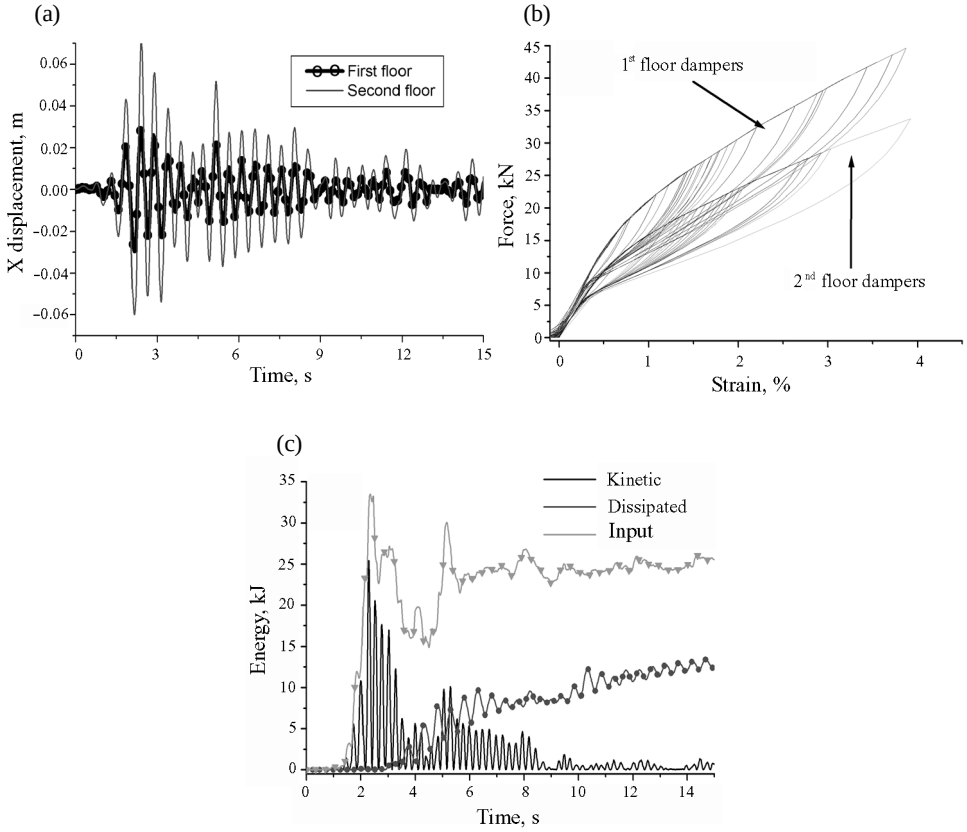

Fig. 16. (a) Oscillation response with the damping system installed. (b) Damper actions during the seismic simulation. (c) Energy evolution in the system.

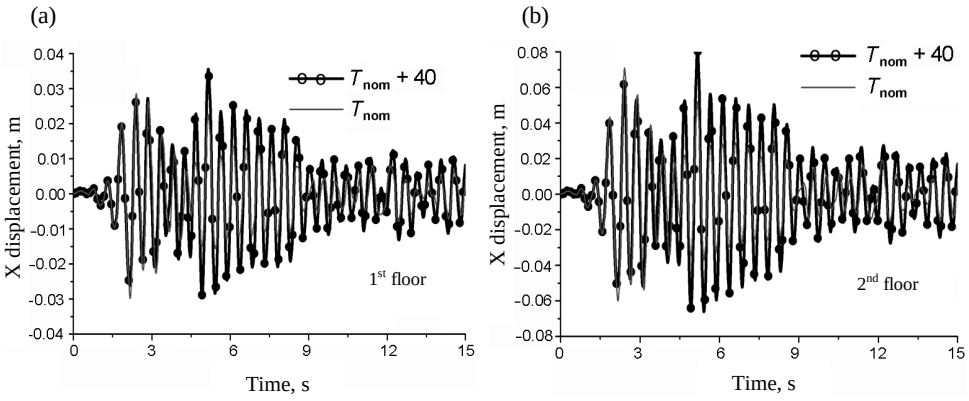

Fig. 17. Response at nominal temperature and at extreme conditions. (a) Oscillation amplitudes on the first floor. (b) Oscillation amplitudes on the second floor.

5.3. Pseudo-semiactive SMA dampers: improving the damping mechanical efficiency

One of the limitations of our dampers is the necessity of minimum oscillation amplitudes in order to dissipate energy. Therefore, small oscillations are not damped by the dampers working in the elastic part. To eliminate this limitation and increase the mechanical efficiency of the dampers, wires with a certain pre-stress can be used. Unfortunately, due to atomic diffusion effects it is not possible to keep the samples in phase coexistence for a long time without degradation. To avoid this problem and still be able to increase the mechanical efficiency, we have devised a mechanical system which is able to use the energy of the earthquake to reduce the wire's length (self-producing a pre-strain). Using this kind of mechanical improvement the long-time reliability of the SMA is maintained and the mechanical efficiency might be improved. Figure 18a,b compare the response with and without pre-strain (the simulation excites the house with the initial 8 s of "El Centro" and shows the relaxation for 8 s without input acceleration). The damping is faster with pre-strain, and as the dissipation appears at very low amplitudes, the damping action is present for more time, dissipating more energy as Fig. 18c shows. The only limitation is time stability of the device, and that these dampers require checking after each event.

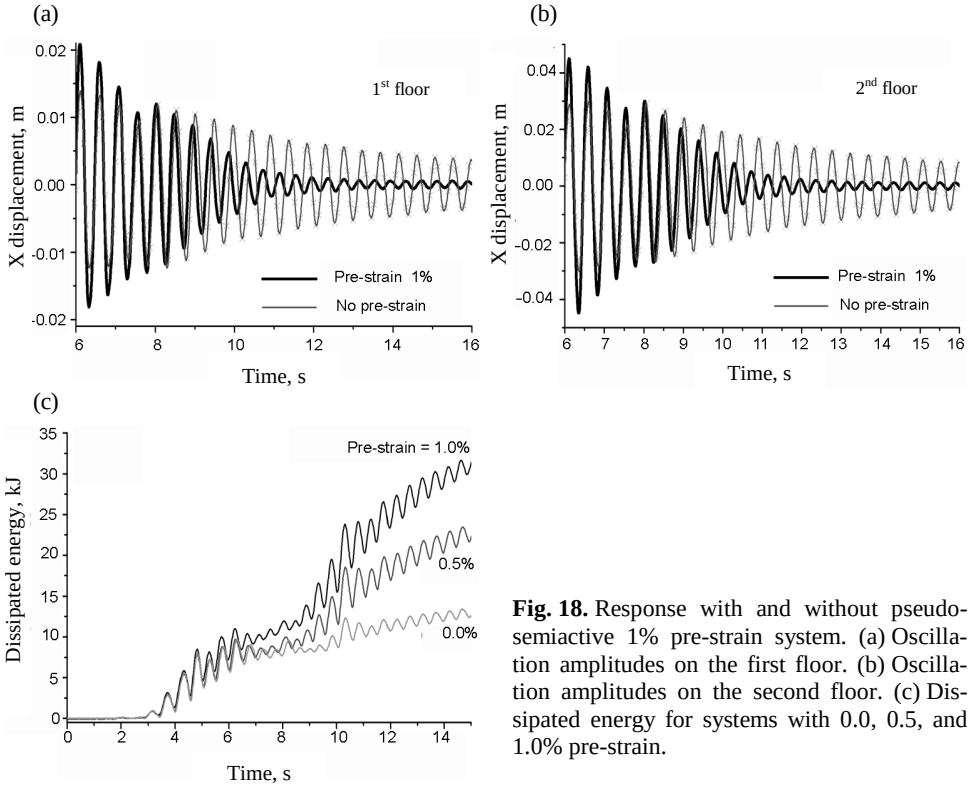

Fig. 18. Response with and without pseudo-semiactive 1% pre-strain system. (a) Oscillation amplitudes on the first floor. (b) Oscillation amplitudes on the second floor. (c) Dissipated energy for systems with 0.0, 0.5, and 1.0% pre-strain.

6. CONCLUSIONS

The Cu-based SMA shows several diffusion effects. Its use in dampers requires that the time effects (or diffusion effects) under the action of stress and/or temperature should be quantified and evaluated according to the application. Preparation of sets of CuAlBe wires requires an initial homogenization at 1123 K, a quench, and ageing. Later, thermomechanical treatment permits the necessary cycles without increase in the SMA creep as required by the application. The CuAlBe alloy is suitable for use in dampers for family houses (forces of the damper close to 30–40 kN). At this preliminary level the NiTi alloy also shows slow effects in time under the action of temperature and stress. The application of this SMA in dampers for civil engineering requires a more detailed study.

ACKNOWLEDGEMENTS

The work was realized in the frame of Spanish projects PCI2005-A7-0254 (MEC) and FPA2000-2635-E (M. de Fomento). Cooperation between CIRG (UPC) and CAB-IB (University of Cuyo, Argentina) has been supported by CNEA and by DURSI (Gen. Catalonia). V. T. thanks Dr. A. Yawny and Mr. H. Soul for support in NiTi analysis. Thanks are due to Mr. Pablo Riquelme for experimental support and Mr. Raul Stuke for creative ideas concerning the development of hand-controlled devices. The collaboration of Mr. S. Ruiz from TA Instruments for the calorimetric measurements in NiTi is gratefully acknowledged.

REFERENCES

1. Lovey, F. C. and Torra, V. Shape memory in Cu-based alloys: phenomenological behavior at the mesoscale level and interaction of martensitic transformation with structural defects in Cu-Zn-Al. *Prog. Mater. Sci.*, 1999, **44**, 189–289.
2. Torra, V., Isalgue, A., Martorell, F., Terriault, P. and Lovey, F. C. From experimental data to quake damping by SMA: a critical experimental analysis and simulation. In *Proceedings of 9th World Seminar on Seismic Isolation, Energy Dissipation and Active Vibration Control of Structures, Vol. 2, Kobe, Japan, June 13–16, 2005*. ASSISI and JAVIT, Tokyo, 241–248.
3. Isalgué, A., Lovey, F. C., Terriault, P., Martorell, F., Torra, R. M. and Torra, V. SMA for dampers in civil engineering. *Mater. Trans*., 2006, **47**, 682–690.
4. Auguet, C., Isalgué, A., Lovey, F. C., Martorell, F. and Torra, V. Metastable effects on martensitic transformation in SMA. Part IV. Thermomechanical properties of CuAlBe and NiTi observations for dampers in family houses. *J. Thermal Anal. Calorimetry*, 2007 (to be published).
5. DesRoches, R., Leon, R. T. and Ocel, J. Testing and analysis of partially restrained connections using SMA dampers. In *Proceedings of 3rd World Conference on Structural Control, Vol. 2, Como, Italy, 2002*. Wiley, Chichester, 2003, 375.

6. Faravelli, L. Experimental approach to the dynamic behavior of SMA in their martensitic phase. In *Proceedings of 3rd World Conference on Structural Control, Vol. 2, Como, Italy, 2002*. Wiley, Chichester, 2003, 163.
7. Collet, M., Foltete, E. and Lexcellent, C. Nonlinear dynamic behaviour of a SMA Experimental and numerical studies. In *Proceedings of 3rd World Conference on Structural Control, Vol. 2, Como, Italy, 2002*. Wiley, Chichester, 2003, 174.
8. Terriault, P., Brailowski, V. and Settouane, K. The benefits of using phenomenological material laws in finite element modelling of SMA structures. In *Proceedings of 3rd World Conference on Structural Control, vol. 2, Como, Italy, 2002*. Wiley, Chichester, 2003, 369.
9. Martorell, F., Isalgue, A., Lovey, F. C., Yawny, A. and Torra, V. Physical constraints in SMA applications. One study case: dampers in civil engineering. In *Proceedings of SPIE, Vol. 5648, Smart Materials 3, 13–15 December 2004, Sidney, Australia* (Wilson, A. R., ed.). Bellingham, Wash., SPIE, 2005, 194.
10. Patoor, E., Lagoudas, D. C., Entchev, P. B., Brinson, L. C. and Gao, X. J. Shape memory alloys. Part I: General properties and modelling of single crystals. *Mech. Mater.*, 2006, **38**, 391–429.
11. Lagoudas, D. C., Entchev, P. B., Popov, P., Patoor, E., Brinson, L. C. and Gao, X. J. Shape memory alloys. Part II: Modelling of Polycrystalls. *Mech. Mater.*, 2006, **38**, 430–462.
12. Saadat, S., Salichs, J., Noori, M., Hou, Z., Davood, H., Bar-on, I., Suzuki, Y. and Masuda, A. An overview of vibration and seismic applications of NiTi shape memory alloy. *Smart Mater. Struct.*, 2002, **11**, 218–229.
13. Peregrina, J. L., Rodriguez de Rivera, M., Torra, V. and Lovey, F. C. Hysteresis in Cu-Zn-Al SMA – From high resolution studies to the time-dependent modeling and simulation. *Acta Metall. Mater.*, 1995, **43**, 993–999.
14. Sutou, Y., Omori, T., Yamauchi, K., Ono, N., Kainuma, R. and Ishida, K. Effect of grain size and texture on pseudoelasticity in Cu-Al-Mn-based shape memory wire. *Acta Mater.*, 2005, **53**, 4121–4133.

Faasi metastabiilsus kujumäluga sulamites ja nende kasutamine ehituses amortisaatoritena

Vicenç Torra, Antonio Isalgué, Francisco C. Lovey ja Ferran Martorell

Kujumäluga sulamite (KMS) erilised omadused on seotud metastabiilsete faaside vaheliste martensiitsete üleminekutega. Nende rakendamine ehituses amortisaatoritena eeldab nende käitumise täielikku mõistmist nii mesoskoopilisel kui ka aatomite tasandil. Esimene tasand on seotud termomehaaniliste omadustega (purunemine, töötsüklite arv, temperatuuriefektid suvel-talvel ja näiteks isesoojenemine, mis on seotud latentse soojuse ning hõõrdejõudude töö poolt tekitatud soojusega). Teine tasand on seotud termodünaamiliste jõudude (tempera

tuur ja rõhk) mõjuga faasiüleminekutele.

On selgitatud CuAlBe sulami omadusi ja kirjeldatud NiTi sulami omi. Kujumäluga sulamite kui amortisaatorite mõju hindamiseks konstruktsioonides on loodud sobiv mudel ja ANSYS-tarkvara kasutades on leitud amortisatsioonivaba ja amortiseeritud konstruktsiooni dünaamilised reaktsioonid maavärina korral, kasutades selleks kirjandusest leitud kiirenduste väärtusi. Järeldustes on esitatud tingimused amortisaatorite omaduste kohta.